Analytical Methods

ROYAL SOCIETY OF CHEMISTRY

PAPER

View Article Online
View Journal | View Issue

Cite this: *Anal. Methods*, 2025, **17**, 1860

Excitation–emission matrix spectroscopy coupled with chemometrics for monitoring ozonation of olive oil and olive pomace oil†

Paula Domínguez-Lacueva,[a] Ewa Sikorska[b] and María J. Cantalejo-Díez*[a]

The effects of ozonation on the Total Polyphenol Content (TPC) of olive oils remain largely unexplored, despite the significant role that polyphenols play in enhancing the health benefits and quality of these oils. Understanding how ozone treatment impacts phenolic compounds is vital, especially considering the documented negative effects of thermal and photochemical oxidation on TPC. The aim of this study was to explore the use of fluorescence spectroscopy combined with chemometrics to develop multivariate models for monitoring the effects of ozonation on TPC and key physicochemical parameters such as the peroxide index (PI), acidity index (AI), iodine value (IV) and viscosity (*V*) in both, virgin and pomace olive oils. Parallel factor analysis and principal component analysis of fluorescence excitation–emission matrices (EEMs) of ozonated olive oils revealed that as the ozonation process progressed, TPC and fluorescence emission decreased. And, at the same time, ozonation increased the values of oxidation indicators such as PI, AI, viscosity and intensity of the Rayleigh scattering signal. PLS models based on analysis of unfolded EEMs exhibited good predictive performance for PI (R^2 = 0.822; RPD > 2.5), and moderate for TPC and V (R^2 = 0.792 and 0.753; RPD > 2). In summary, we demonstrated the feasibility of EEM spectroscopy for monitoring the ozonation process. The use of this method can ease the characterization of ozonated olive oils and, additionally, make the analysis more sustainable.

Received 18th December 2024
Accepted 14th January 2025

DOI: 10.1039/d4ay02267j

rsc.li/methods

1 Introduction

Ozonated olive oils have gained attention in recent years due to their unique antimicrobial properties[1] and health benefits.[2] Combining the antioxidant-rich nature of olive oil with the oxidative power of ozone, these formulations present potential applications in both the food industry and clinical therapies. One of the main drawbacks of ozone (O_3) is its high reactivity, which contributes to the molecule's instability. However, the reaction between the double bonds (C=C) of olive oil's unsaturated fatty acids with O_3 results in the formation of compounds such as aldehydes, ketones and peroxidic species[3] that retain the bactericidal and curative properties of ozone[4] in addition to making them more stable.[5]

The quality of the ozonation process of olive oil depends on different factors such as O_3 concentration, ozonation time, temperature and the composition of the selected olive oil.[6] Depending on the lipid profile and the level of unsaturation of the selected olive oil, ozonation will produce organic compounds of a different nature. Therefore, depending on the initial quality[7–9] of the olive oil (refined, virgin or extra virgin olive oil), the effectiveness of the resultant ozonated olive oil may vary. The high content of unsaturated fatty acids is one of the most important characteristics to take into account when choosing olive oil for ozonation.[10] An interesting alternative may be to use pomace olive oil, a by-product obtained through the extraction process of extra virgin olive oil, in this process. In fact, pomace olive oil has a high oleic acid and polyphenol content[11] which, to our knowledge, has not yet been used for ozonation.

Accordingly, monitoring the ozonation process is a crucial step in the elaboration of these oils. The traditional methodologies used for physicochemical characterization of ozonated oils are time-consuming, require the use of several chemical reagents and provide limited information about the chemical changes that occur in oils during the ozonation process. Among the physicochemical parameters used for the assessment of the quality of ozonated olive oils, the peroxide index (PI, reflecting the production of oxidation products), acidity index (AI, indicating the free fatty acid content), iodine value (IV, assessing unsaturation levels) and viscosity (V, determining fluidity) are the most common and studied ones.[6] However, there is little or no information about the effect of ozonation on the Total Polyphenol Content (TPC) of ozonated olive oils. The

[a]*Institute for Sustainability & Food Chain Innovation (IS-FOOD), Public University of Navarre (UPNA), Arrosadia Campus, E-31006 Pamplona, Spain. E-mail: iosune.cantalejo@unavarra.es*

[b]*Institute of Quality Science, Poznań University of Economics and Business, al. Niepodległości 10, 61-875 Poznań, Poland*

† Electronic supplementary information (ESI) available. See DOI: https://doi.org/10.1039/d4ay02267j

importance of polyphenols cannot be overstated, as these compounds play a crucial role in contributing to olive oil's health-promoting properties[12–14] and overall quality.[15–17] There is scientific evidence about the negative effects of thermo-[18–21] or photo-[22–24]oxidation on the TPC of olive oils. Therefore, it is crucial to study how O_3 affects the phenolic content of olive oils, in order to assess the presence of these valuable compounds in ozonated olive oil's formulations.

Techniques that operate directly on almost unaltered samples, without the need for a long tedious pre-treatment, are valuable for routine control tasks, especially when handling a substantial number of samples. Spectroscopic methods, coupled with chemometrics, meet this criterion[25] and are successfully used to test the quality of olive oil.[26] These methods involve creating multivariate calibration models by utilizing the spectral characteristics of samples and reference values for the target analyte obtained through traditional analytical approaches. The established regression models facilitate the quantification of analytes solely based on their spectral signatures. Several authors have already proved the use of spectroscopic techniques such as ^{1}H-NMR,[5,8] NMR[27,28] and FT-IR[29] to monitor the ozonation process. The main objective of all the previous studies was to identify and quantify the formation of new compounds such as ozonides (1,2,4-trioxolane), aldehydes and other molecules with shorter carbon chains.

Spectrofluorimetric techniques emerge as a rapid, accurate and sustainable tool for food analysis and quality assessment[30] offering a unique opportunity for the characterization of olive oils. The information provided by the excitation–emission matrix (EEM) fluorescence spectroscopy allows a comprehensive exploration of the fluorescence properties of olive oils,[31] shedding light on crucial parameters such as polyphenol content,[32] oxidation status,[33] and overall quality.[34] However, these techniques have not been used so far to study the olive oil ozonation process. The present study aims to evaluate the possibility of using fluorescence spectroscopy coupled with chemometrics to create multivariate models that would allow the monitoring of the effect of ozonation on the TPC in addition to monitoring the changes in the most relevant physicochemical parameters (PI, AI, IV and V) of virgin olive oil and pomace olive oil.

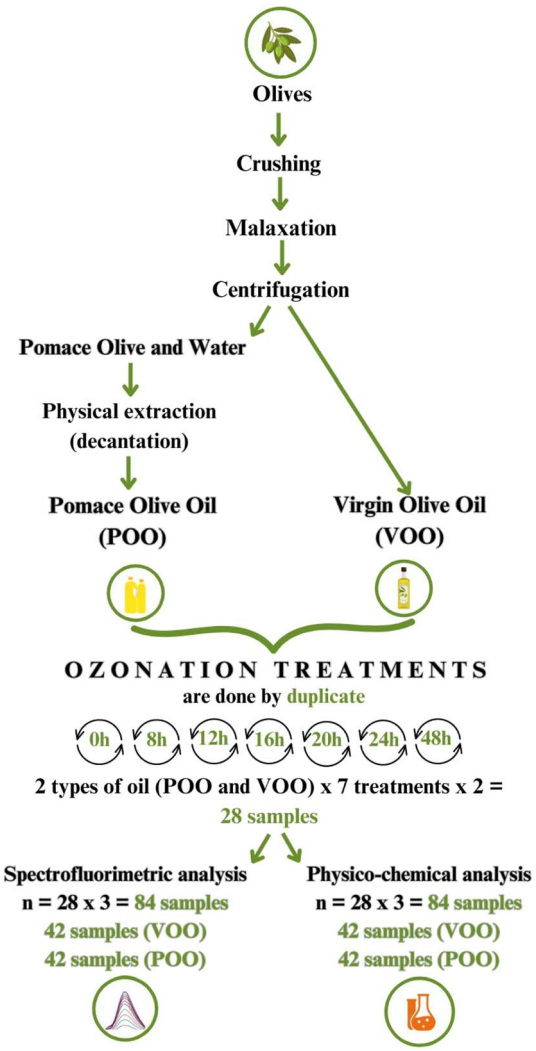

Fig. 1 Flowchart representation of the experimental design followed in this study.

2 Materials and methods

2.1. Ozonated olive oils

The ozonation process was carried out on two different olive oils: Virgin Olive Oil (VOO) and Pomace Olive Oil (POO), produced by the company Biosasun S.A. (Allo, Spain). The POO used is a type of olive oil that was mechanically extracted from the leftover residue (pomace) after the first press. Both oils were obtained from the variety *Olea europaea* L. For the study, six ozone treatments of different durations (8, 12, 16, 20, 24, and 48 hours) were conducted, along with a control without ozone exposure (0 hours). All treatments were carried out in duplicate on 40 mL of oil, adding up to a total of 84 samples to analyse. Each ozone treatment was performed using OXITRES (Toledo, Spain) equipment from the AF-C series, specifically, the AF1000C model with a production of 1 g of O_3/hour at 20 °C. The ozonated oils were stored for 24 hours in a refrigerator at 4 °C after the ozonation process. The experimental design followed in this study is presented in Fig. 1.

2.2. Reagents

Chloroform (≥99,8%), glacial acetic acid (≥99%), cyclohexane (≥99,8%), diethyl ether (≥99%), methanol (≥99,8%), and potassium hydroxide were purchased from Fisher Chemical (Madrid, Spain). Potassium iodide (99%) was purchased from Thermo Scientific (Madrid, Spain). Starch, *n*-hexane (99%), heptane (99%), sodium thiosulfate (0.01 M) and phenolphthalein were purchased from Sharlab (Barcelona, Spain). Ethanol was purchased from Oppac (Noain, Spain).

2.3. Physicochemical analyses

All physicochemical analyses were performed in triplicate and the ozonated olive oils were analysed 24 hours after the ozonation process. The Fatty Acid Methyl Ester (FAME)

determination, Peroxide Index (PI), Acidity Index (AI), Iodine Value (IV) and Total Polyphenol Content (TPC) assays were carried out according to the methodologies described by the International Olive Council.[35]

2.3.1. Fatty Acid Methyl Ester (FAME) determination. All ozonated olive and pomace oil samples were purified prior to gas chromatography (GC) analysis of Fatty Acid Methyl Esters (FAMEs). For the purification, a HyperSep Silica cartridge (Thermo Scientific, Madrid, Spain) was placed in a vacuum elution apparatus and washed with 6 mL of hexane. Then a solution of the oil (0.12 g approximately) in 0.5 mL of hexane was loaded onto the column. The solution was pulled down and then eluted with 10 mL of hexane/diethyl ether (87 : 13 v/v). The combined eluates were homogenised and an aliquot was evaporated to dryness in a rotary evaporator under reduced pressure at room temperature. The residue was dissolved in 1 mL of heptane for fatty acid methyl ester preparation and analysis by GC. The preparation of the fatty acid methyl esters from ozonated and non-ozonated olive oils and olive pomace oils was performed by trans-esterification with methanolic solution of potassium hydroxide at room temperature. In a 5 mL screw-top test tube, 0.1 g of the purified oil sample was weighed. Then, 2 mL of heptane and 0.2 mL of the methanolic potassium hydroxide solution (2 M) were added. The solution was shaken vigorously for 30 seconds. We left the solution to stratify until the upper layer became clear. The upper layer contained the methyl esters ready for injection into the gas chromatograph. A Hewlett–Packard/Agilent 5890 Series II Gas Chromatograph with FID was used for the quantitative analysis of FAMEs. Together with helium as a carrier gas, a Teknokroma SupraWAX-280 Capillary Column of 30 m × 0.53 mm × 1 μm was employed for the analysis. The injector and detector were preheated to 250 °C and then the oven was set to 165 °C. For the determination, 1 μL of diluted samples (1 : 10) were manually injected using a Hamilton glass syringe of 5 μL. Once the analysis began, the oven temperature was maintained at 165 °C for 2 minutes and increased to 250 °C at a speed of 2 °C min^{-1}. The total flow established for the analyses was 2 mL min^{-1}.

2.3.2. Peroxide index (PI). To calculate the PI, 0.5 g of the sample was weighed into a flask and 10 mL of chloroform and 15 mL of acetic acid were added to dissolve the oil. Then, 1 mL of a saturated solution (14 g/10 mL) of potassium iodide was added and it was left in the dark for 5 minutes. After that, 75 mL of distilled water was added and the iodine released was titrated using a 0.5 M sodium thiosulphate solution with starch as an indicator.

2.3.3. Acidity index (AI). For the analysis, 0.5 grams of sample were weighed and dissolved in a 50 mL mixture of diethyl ether and ethanol at 95% (v/v), previously neutralised. The solution was titrated with 0.1 M potassium hydroxide solution until the phenolphthalein indicator turned to pink colour for at least 10 seconds.

2.3.4. Iodine Value (IV). The determination of the iodine value was carried out by weighing 0.2 g of the sample into a 500 mL flask and adding 20 mL of a solvent previously prepared with equal volumes of cyclohexane and acetic acid. Then, 25 mL of Wijs reagent was added and the mixture was left for 2 hours in the dark. When the time had passed, 20 mL of a potassium iodide solution (100 g L^{-1}) and 150 mL of distilled water were added. The solution was titrated with a 0.01 M sodium thiosulphate solution using starch until the blue colour disappeared.

2.3.5. Total Polyphenol Content (TPC). For the sample preparation step, we weighed 2.0 g of olive oil into a 10 mL screw-capped test tube. Then, 5 mL of an extraction solution of methanol/water 80 : 20 (v/v) was added, followed by 1 minute of shaking. The mixture underwent ultrasonic extraction for 15 minutes at room temperature, followed by centrifugation at 5000 rpm for 25 minutes. Then, 0.5 mL of the collected supernatant was mixed with 2.5 mL of Folin–Ciocalteu reagent, followed by a 5 minute rest. Next, a solution of 75 g L^{-1} sodium carbonate was added and the samples were incubated for 1 hour at room temperature. Absorbance was measured at 765 nm, and the results were expressed as grams of gallic acid equivalents (GAE) per kg of dry mass.

2.3.6. Viscosity (*V*). Viscosity (V) measurements were performed using a HAAKE K15 Rotovisco 1 viscosimeter using a Z20 DIN rotor. Measurements were also performed in triplicate by using 7 mL of oil in a continuous ramp from 0–500 Pa at 25 °C.

2.4. Fluorescence measurements

Fluorescence spectra were recorded using a Cary Eclipse Fluorescence Spectrometer (Agilent Technologies, USA). The total fluorescence spectra (excitation–emission matrices, EEMs) were obtained by recording the emission spectra in the wavelength range from 300 to 800 nm (at 10 nm intervals) with the excitation wavelengths ranging between 250 and 400 nm, at 10 nm intervals. The excitation and emission slit widths were 1.5 and 1 nm, respectively. The samples were diluted (1% v/v) in *n*-hexane for the analysis. Measurements were carried out in triplicate.

2.5. Data analysis

Parallel factor (PARAFAC) analysis was performed to decompose the EEMs of both olive oils (VOO and POO) and see the contributions of individual fluorescent components.[36] A three-way data array with a size of 84 × 16 × 51 (number of samples × number of excitation wavelengths × number of emission wavelengths) was used in the PARAFAC analysis. The emission from *n*-hexane was removed by subtracting the emission spectra of the solvent before the analysis. The Rayleigh scattering signals were removed by inserting the missing values in the bands centered on the wavelength identity line ($\lambda_{ex} = \lambda_{em}$). Non-negativity constraints that assumed non-negative values for both the excitation and emission spectral profiles and the concentrations were applied, so that meaningful results were obtained. Core consistency (CORCONDIA) and split-half analysis were performed to find the optimal number of components in the PARAFAC models.[36]

Principal component analysis (PCA) was performed to visualize the changes in the overall quality of olive oils during ozonation and to explore the relationship between

physicochemical parameters and fluorescence data. PCA was performed on the X matrix, which contained physicochemical parameters and scores of fluorescent components obtained from the PARAFAC analysis. The X data were scaled prior to analysis.

Partial least squares (PLS) regression and *N-way* PLS (NPLS) regression were used to model the relationship between the fluorescence data (the X matrix) and the analytical parameters (TPC, PI, AI, IV, and V) in the Y matrix. The PLS method models both the X and Y matrices simultaneously, finding the latent variables in X that best predict the latent variables in Y.[37] The data pre-processing included mean-centering over the sample mode. The data set used for analyses was a combination of EEMs from both oils (VOO and POO). The NPLS analysis was performed on the EEMs arranged into three-way arrays with a size of 84 × 16 × 51 (number of samples × number of excitation wavelengths × number of emission wavelengths). The PLS analysis was performed on the unfolded array with dimensions of 84 × 816 (number of samples × number of excitation wavelengths × number of emission wavelengths). To obtain the unfolded data set, the three-way EEMs were unfolded along the sample mode. The PLS was also used on the matrix consisting of the score data obtained from the PARAFAC model with the four components and Rayleigh scattering signal, with dimension (84 × 5). The Variable Importance in Projection (VIP) was used to select important variables that contribute significantly to these models.[38]

The development of multivariate calibration models included the following steps: (i) selection of training and test sets; (ii) building a model using the samples that constitute the training set; and (iii) validation of the model using the test set.[37] All the studied samples were divided into the training set (56 samples) and the test set (28 samples) using the Onion algorithm. The venetian blinds variant of cross-validation with five data splits was used for all the models. The optimal number of components was chosen as the minimum for the plot of the root-mean-square error of the cross-validation (RMSECV) as a function of the number of components. The independent test set was used for the external validation. The regression models were evaluated using the determination coefficients (R^2), the RMSECV, the root-mean-square error of prediction (RMSEP) and the relative predictive deviation (RPD) calculated as the ratio of the standard deviation for the reference data to the RMSECV or RMSEP.[39] The data analysis was performed using Solo v. 5.0.1 software (Eigenvector Research Inc., USA).

3 Results and discussion

3.1. Ozonation effect on the physicochemical characteristics of VOO and POO

Fatty acid quantification analyses with GC-FID were carried out with the aim of evaluating the lipid profile of both oils (VOO and POO) before and after the ozonation process.

As evident from Table 1 both oils had a similar initial lipid profile before undergoing the ozonation process. There were no significant differences in the composition of the four fatty acids (palmitic, stearic, oleic and linoleic acids) studied. In accordance with previous results,[40,41] pomace olive oils retain high oleic acid content since they come from the same olives as virgin olive oil. Once the ozonation process was carried out, the analysis was performed again in both oils with the aim of measuring the reduction in the fatty acid content after the ozonation process. As was expected, the main reduction was observed in the oleic acid content; this reduction was 69% and 47% for VOO and POO, respectively. According to previous results,[9] this is the result of the ozonation process itself, as a consequence of the reaction between O_3 and the double bonds in the oleic acid. Given that the double bonds present in oleic acid are one of the most important factors to take into account in the ozonation process of vegetable oils,[7–9] the results obtained (Table 1) suggest that pomace olive oil can potentially be used for ozonation. The differences between the physicochemical parameters of both oils before and during ozonation treatments are presented in Fig. 2.

The highest peroxide indexes were achieved after 48 h of ozonation in both oils (Fig. 2a); the values were 1233.27 and 1871.11 mEq O_2 per kg for VOO and POO, respectively. It has been previously demonstrated[9] that the diverse oxidation products (ozonides, aldehydes and peroxides) produced during ozonation, in addition to increasing the PI, contribute significantly to the acidification of olive oils. Thus, acidity values also increased in both oils after ozonation. Nevertheless, the values were almost twice as high in POO than in VOO; 7.80° (POO) and 4.77° (VOO) were the highest values achieved after 48 hours of ozonation (Fig. 2b). The iodine value of VOO decreased from 97.18 to 52.76 g I/100 g oil (Fig. 2c), indicating a reduction of 45.7% of the unsaturation. In contrast, POO reduced its unsaturation level by 53.2%, decreasing from 90.56 to 43.01 g I/100 g oil. Considering that both oils had similar initial lipid profiles (Table 1), unsaturation levels evolved in a similar way in both oils.

The correlation between the ozonation time and the reduction in the TPC demonstrated that the oxidation process derived

Table 1 Results of the quantification of palmitic, stearic, oleic and linoleic acid methyl esters represented in g kg^{-1} of virgin olive oil and pomace olive oil before and after ozonation. Results showed as mean values ± s.d

Olive oil	Ozonation	Palmitic acid (C16:0)	Stearic acid (C18:0)	Oleic acid (C18:1, *cis*-9)	Linoleic acid (C18:2, *cis*, *cis*-9, 12)
Virgin olive oil	Not O_3	10.84 ± 0.68	4.69 ± 0.23	76.56 ± 4.68	9.13 ± 0.65
	48 h O_3	9.24 ± 1.11	4.45 ± 1.18	24.01 ± 4.04	7.23 ± 0.58
Pomace olive oil	Not O_3	11.73 ± 0.55	4.11 ± 0.17	77.35 ± 0.75	8.96 ± 0.32
	48 h O_3	8.52 ± 0.76	3.15 ± 0.04	41.23 ± 4.64	3.34 ± 0.36

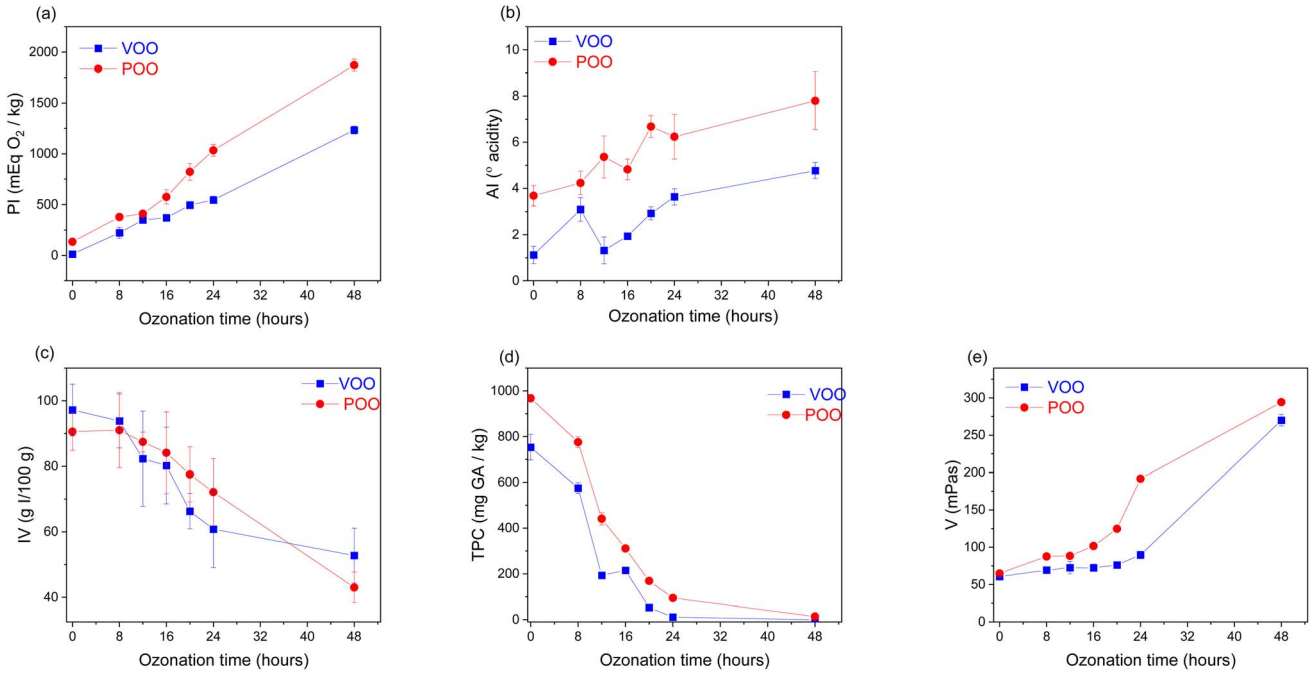

Fig. 2 The evolution of the selected physicochemical parameters of virgin (VOO) and pomace (POO) olive oils according to the ozonation time (hours) and oil type, where: (a) peroxide index (PI), (b) acidity index (AI), (c) iodine value (IV), (d) total polyphenol content (TPC) and (e) viscosity (*V*); the mean value and standard deviation for each ozonation time are presented.

from ozonation significantly affects the polyphenols present in the olive oils. The entire set of VOO samples studied had TPC in the range between 598.76 (8 h) and 0.00 (not detected) (48 h) mg GA kg; whereas the set of POOs showed TPCs between 798.76 (8 h) and 7.19 (48 h) mg GA kg^{-1} (Fig. 2d). In the case of VOO, the reduction in the TPC was 100%; whereas, for POO, the reduction from 8 to 48 hours of ozonation resulted in a reduction of 99.1% in the TPC. Due to their hydrophilic nature, phenolic compounds were more abundant in pomace than in virgin olive oil, since it is known that only a fraction is transferred to olive oil during oil extraction,[42] whereas most of them remain in the by-product.

Finally, it was seen that the viscosity of the oils increased with ozonation time. The breakdown of the C=C double bonds together with the effect of the O_3 gas in increasing the attractive forces between the saturated hydrocarbon molecules of the oil,[43] are responsible for this outcome. POO turned out to be more viscose than VOO, achieving viscosity values of almost 300 (294.69) mPas (Fig. 2e).

3.2. Ozonation effect on the fluorescence of VOO and POO

In order to obtain comprehensive characteristics of the fluorescence of studied oils and to evaluate the changes of fluorescent components during the ozonation process, we recorded the EEMs for the entire set of samples studied. Fig. 3 presents the contour maps of EEMs of fresh VOO and POO and the samples ozonated for 16 and 48 hours. The EEMs of fresh POO and VOO showed intense emission bands in the excitation wavelength range of 280–360 nm and emission wavelength range of 300–500 nm. Emission in this range is characteristic for olive oils and is related mainly to polyphenols and tocopherols. Oxidation products in olive oil may also emit in this spectral range.[44,45] The emission of VOO is dominated by the band with a maximum at $\lambda_{ex}/\lambda_{em}$ of 310/330 nm. In the EEMs of POO, two emission bands are present with maxima at $\lambda_{ex}/\lambda_{em}$ of 295/310 nm and 320/410 nm. The observed noticeable differences in fluorescence of both oils may indicate different compositions of polyphenols and tocopherols, and the presence of some fluorescent components related to the oil processing.

The most significant difference between the EEMs of non-ozonated VOO and POO was observed in the long wavelength region. The intense emission band with a maximum at $\lambda_{ex}/\lambda_{em}$ of 400/675 nm present only in spectra of VOO, corresponds to the fluorescence of chlorophyll pigments, mainly pheophytins. The absence of pheophytin emission in EEMs of POO makes evident the different nature of both oils. Pigments such as chlorophyll or carotenoids are widely used as indicators to determine the quality of olive oils.[46] These appear in large quantities in virgin or extra virgin olive oils and, in contrast, are scarce or absent in pomace or refined oils. In fact, chlorophyll fluorescence is a rapid methodology used in the olive oil industry to detect adulterations.[47]

Ozonation caused a gradual decrease in the emission intensity of all bands, both for ozonated VOO and POO. However, none of the oils showed new emission bands as the ozonation time increased, suggesting that the oxidation products formed during ozonation do not show any fluorescence. In addition to the fluorescence bands of oil components, a signal from Rayleigh scattering is visible in EEMs, presented in Fig. 3. These intense peaks occur at excitation wavelengths equal to the emission wavelengths. They act as interferents in EEM

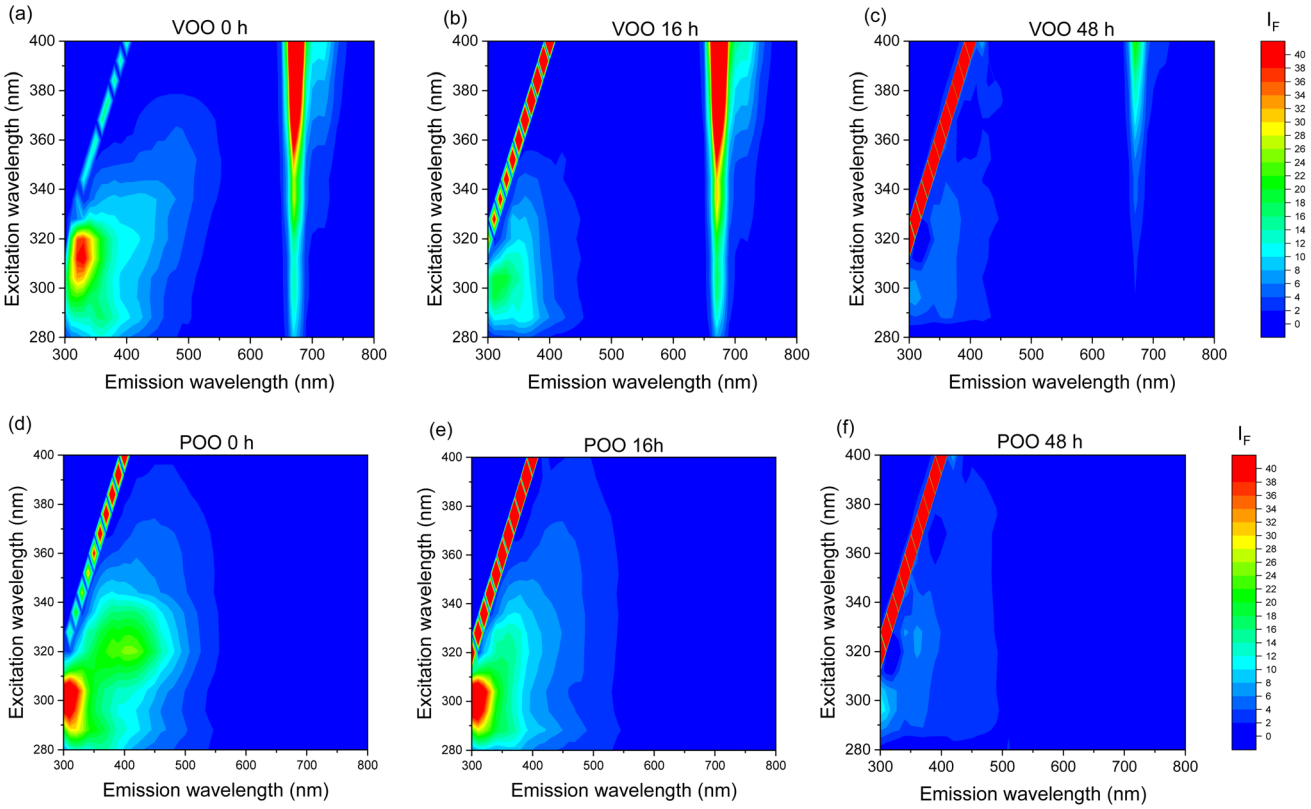

Fig. 3 Contour maps of the excitation–emission matrices (EEMs) of virgin (VOO) and pomace (POO) olive oils. Top panel: VOO (a) non-ozonated, (b) ozonated for 16 h, and (c) ozonated for 48 h. Bottom panel: POO (d) non-ozonated, (e) ozonated for 16 h, and (f) ozonated for 48 h. EEMs are presented on the same fluorescence intensity scale.

measurements and are usually removed before further multivariate analysis of the spectra. However, in our studies we noticed that the intensity of the Rayleigh scattering signal increased with the ozonation time of the oils; therefore, in further analyses, we additionally examined the effect of treatment of oils on the intensity of these peaks.

3.3. PARAFAC for monitoring the ozonation effect on the fluorescence of VOO and POO

In order to investigate the effect of ozonation on fluorescent oil components we used the PARAFAC multiway exploratory method. The analysis was performed with the objective of resolving the entire set of EEMs of VOO and POO into contributions of individual fluorescent compounds. An optimal PARAFAC model with four components was identified based on the core consistency diagnostic, inspection of both the residuals and loadings and half-split analysis. Fig. 4 presents the contour maps of excitation–emission profiles of extracted fluorescent components and their evolution during the ozonation process.

Taking into account the diversity of polyphenols present in olive oil and the similarity of fluorescence properties within the same groups of compounds,[48] it should be stated that the components obtained as a result of the PARAFAC analysis correspond to groups of substances with similar properties rather than to individual chemical compounds. The first component extracted by the PARAFAC model had a $\lambda_{ex}/\lambda_{em}$ maximum at 400/675 nm, corresponds to pheophytins, and is present only in VOO. The next three components may be related to different classes of phenolic compounds. The second component showed its $\lambda_{ex}/\lambda_{em}$ maximum at 295/315 nm, and may correspond to phenolic compounds mainly from the secoiridoids group. The third component with $\lambda_{ex}/\lambda_{em}$ maxima at wavelengths of 290, 320/400 nm, may be related to the fluorescence of some benzoic and hydroxycinnamic acids. The fourth component with $\lambda_{ex}/\lambda_{em}$ maxima at 290, 310/330 nm may correspond to tocopherols, with contributions of phenols including some simple phenolic alcohols.[45,48,49]

The contributions of each of the four fluorescent components to the EEMs of oil samples are presented in Fig. 4(e)–(h) as the mean of score values obtained in the PARAFAC decomposition for each ozonation time. The ozonation resulted in a gradual decrease of the scores of PARAFAC components 2, 3, and 4, related to polyphenols and tocopherols, for both ozonated VOO and POO. This observation is consistent with the results of chemical analysis, which showed a decrease in the TPC during ozonation. Additionally, in the case of VOO, there was also a significant reduction in the score of component 1, ascribed to the emission of pheophytins. It is well-known[50] that ozonation removes the green colour of olive oil until it becomes white-yellowish.

It should be noted that using the PARAFAC analysis we did not extract any component with increasing intensity in the

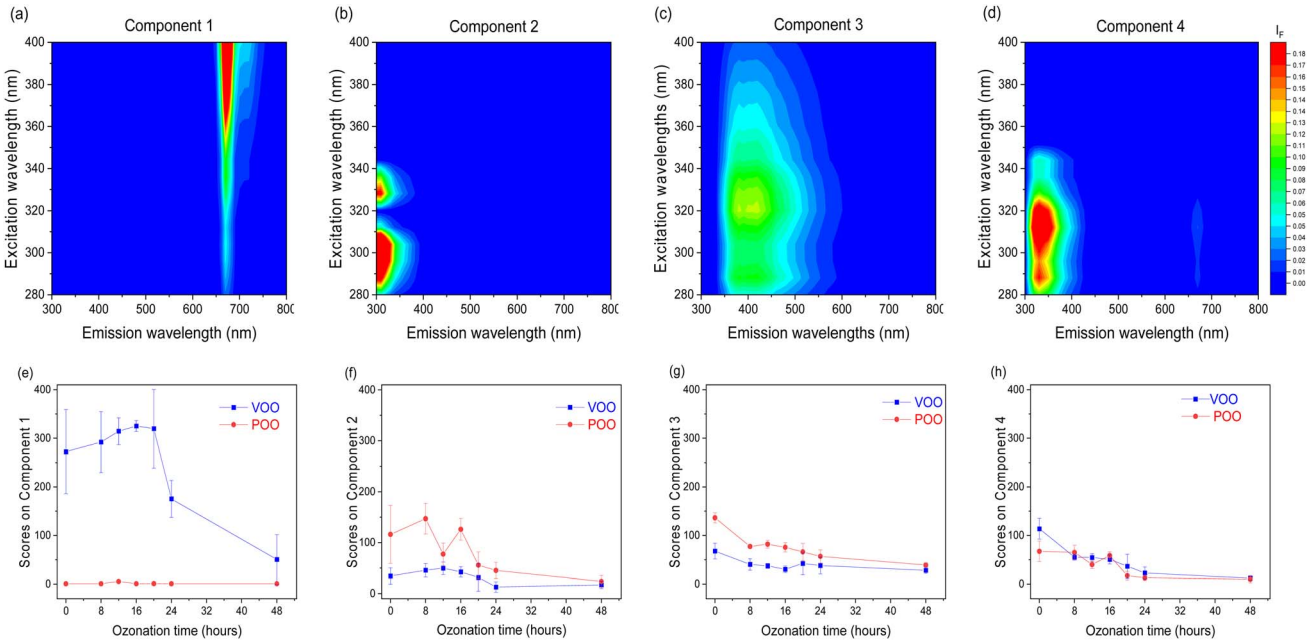

Fig. 4 Results of PARAFAC analysis of the three-way EEM array of virgin (VOO) and pomace (POO) olive oil samples. Top panel: (a)–(d) excitation–emission profiles of fluorescent components 1–4, respectively. Bottom panel: (e)–(h) the evolution of the fluorescent components 1–4 according to the ozonation time (hours) and oil type, the mean value and standard deviation of scores for each ozonation time are presented.

intermediate emission region (400–600 nm), where oxidation products usually emit fluorescence.[45] It can therefore be concluded that, unlike thermal and autoxidation, ozonation does not lead to the formation of fluorescent products due to a different mechanism of this process. This conclusion matches with the hypothesis of other authors,[6] suggesting that the reaction between O_3 and the fatty acids present in olive oil produces a series of oxidation compounds of a different nature to those produced naturally during oil storage.

3.4. Correlation between physicochemical and fluorescence data

In order to evaluate the overall changes in the properties of oils during the ozonation process, principal component analysis (PCA) was performed. The X matrix used for PCA included all physicochemical parameters, PARAFAC scores for the four extracted fluorescent components, and intensity of the Rayleigh scattering signal. The PCA results as the bi-plot are presented in Fig. 5.

The first principal component PC1, which describes 60% of the total data variance, revealed the changes in oil characteristics during the ozonation process as a function of time. Fresh oil samples are characterized by relatively high TPC content, IV value and fluorescence intensity of all four components extracted using the PARAFAC method. As the ozonation process progressed, these parameters decreased, and at the same time increased the values of oxidation indicators such as PI, AI, viscosity and intensity of the Rayleigh scattering signal.

It is worth mentioning that both ozonized olive oils (VOO and POO) showed some significant differences in physicochemical and spectral data; and this was confirmed by the results obtained using PCA (Fig. 5). The second principal component, PC2, which described 27% of the total data variance, differentiated the two oil categories, VOO and POO. POO samples were characterized by higher TPC content, AI value and scores of fluorescent components 2 and 3, while VOO had considerably higher scores on fluorescent component 1 (chlorophylls). Nevertheless, once the

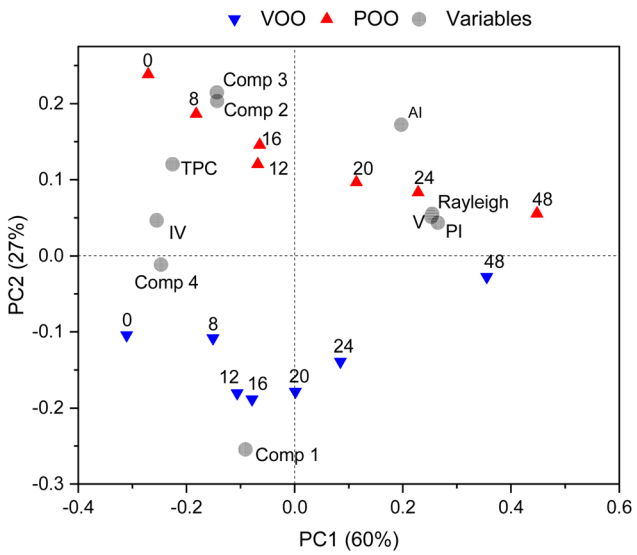

Fig. 5 Bi-plot of the results of principal component analysis (PCA) of the physicochemical and fluorescent properties of extra virgin olive oil (VOO) and pomace olive oil (POO) samples subjected to ozonation. Abbreviations: peroxide index (PI), acidity index (AI), iodine value (IV), total polyphenol content (TPC), viscosity (*V*); scores of four fluorescent components obtained using PARAFAC (Comp 1, Comp 2, Comp 3 and Comp 4), intensity of Rayleigh scattering (*R*); numbers from 0 to 48 indicate ozonation time in hours.

ozonation treatment was finished, both oils appeared to be similar in terms of the tested parameters.

Analysis of PCA loadings revealed the correlations that occurred between the analytical parameters and the scores of the fluorescent components obtained in PARAFAC. This correlation was also evident from calculated Pearson coefficients (ESI, Fig. S1†). Positive correlations ($r > 0.5$) were observed between TPC and fluorescent component 2 ($r = 0.584$), component 3 ($r = 0.697$) and component 4 ($r = 0.727$). Fluorescent component 1 is negatively correlated with the AI value ($r = -0.747$, p). Fluorescent component 4 is negatively correlated with PI ($r = -0.721$), AI ($r = -0.622$), viscosity ($r = -0.628$), and Rayleigh scattering intensity ($r = -0.677$), and positively ($r = 0.650$) with IV. It should be noted that only correlations between fluorescent components and TPC may be considered direct. Because emission from ozonation products was not observed in the EEMs, other correlations were indirect and were a consequence of correlations between phenol, tocopherol and pheophytin content and respective analytical parameters.

Table 2 Characteristics of the training and test sets used for the discrimination and regression models for TPC, PI, AI, IV, and V of the olive oils studied. The number of samples in the training and prediction sets was $n = 56$ and $n = 28$, respectively

Analytical parameter	Set	Range	Mean	SD
TPC (mg GA kg^{-1})	Training	0–988.29	347.74	330.96
	Test	0–960.30	285.09	280.26
PI (mEq O_2 kg^{-1})	Training	7.09–1907.40	558.18	417.24
	Test	8.34–1940.36	695.94	584.97
AI (°acidity)	Training	0.78–7.07	3.89	1.79
	Test	0.79–9.85	4.55	2.37
IV (g I/100 g)	Training	37.57–112.16	78.57	17.61
	Test	37.64–102.04	74.09	19.33
V (mPa s)	Training	60.62–295.30	112.51	67.74
	Test	59.33–296.24	131.55	86.83

Interestingly, the intensity of the Rayleigh scattering signal was positively correlated with viscosity ($r = 0.919$), PI ($r = 0.867$), AI ($r = 0.653$), and negatively correlated with IV ($r = -0.638$) and scores of fluorescent component 4 ($r = -0.678$). This phenomenon could suggest that the changes in the composition of olive oil after the ozonation process, and the subsequent formation of new compounds, affect not only the chemical parameters of oils (AI and PI) but also their physical characteristics. It has been already demonstrated[51] that changes in the structure, density and composition of food matrices could affect the Rayleigh scattering; but there is no prior information about the effect of ozonation in this phenomenon.

3.5. Calibration models

As a next step, we studied the possibility of using fluorescence to assess the reduction of TPC during ozonation in the olive oils studied. This would permit the estimation of the disappearance ratio of the polyphenol compounds as ozonation time increases, and study the effect of oxidation produced by O_3. The entire dataset of both oils together (VOO and POO) was split into a training set used for the model development, and a test set used for external model validation. The statistics for the training and test sets are presented in Table 2.

Multivariate PLS regression was used to model the quantitative relations between the VOO fluorescence and TPC. The same analyses were performed for the other analytical parameters (PI, AI, IV and V) in order to see whether it was possible or not to model the effect of ozonation on these values, even indirectly. Different variants of PLS regression were applied depending on the structure of the analysed data. The NPLS variant was used for the analysis of the EEMs arranged into a three-way array. The ordinary PLS regression variant was applied to analyse the unfolded EEMs and to analyse the matrix consisting of the scores of the four fluorescent components obtained from the PARAFAC model and the Rayleigh scattering

Table 3 Characteristics of regression models for the prediction of TPC, PI, AI, IV, and V in both ozonated virgin olive oil (VOO) and pomace olive oil (POO); calibration, cross-validation ($n = 56$ samples) and prediction ($n = 28$ samples)[a]

Parameter	PLS model	LV	R^2_C	RMSEC	R_{CV}^2	RMSECV	R_P^2	RMSEP	RPD_P
TPC	NPLS	6	0.896	105.98	0.843	132.13	0.787	127.73	2.2
	PLS	4	0.847	125.85	0.801	144.37	0.792	132.09	2.1
	PLS-PARAFAC-R	3	0.866	119.90	0.842	130.52	0.612	175.06	1.6
PI	NPLS	4	0.824	173.17	0.748	207.99	0.752	321.13	1.8
	PLS	6	0.848	195.17	0.730	261.11	0.822	163.70	3.6
	PLS-PARAFAC-R	3	0.832	169.72	0.802	184.02	0.791	291.29	2.0
AI	NPLS	7	0.833	0.72	0.758	0.88	0.724	1.36	1.7
	PLS	5	0.777	0.922	0.711	1.05	0.793	1.41	1.7
	PLS-PARAFAC-R	3	0.753	0.881	0.712	0.954	0.773	1.309	1.8
IV	NPLS	5	0.629	10.36	0.537	11.66	0.562	12.85	1.5
	PLS	5	0.693	10.14	0.579	11.99	0.539	10.45	1.8
	PLS-PARAFAC-R	3	0.543	11.50	0.483	12.27	0.549	13.02	1.5
V	NPLS	6	0.871	24.13	0.779	31.90	0.723	46.34	1.9
	PLS	6	0.847	30.21	0.725	40.79	0.753	35.27	2.5
	PLS-PARAFAC-R	3	0.898	21.41	0.868	24.40	0.801	38.87	2.2

[a] LV – number of latent variables used for regression; R_C^2, R_{CV}^2, and R_P^2 – determination coefficient for calibration, cross-validation, and prediction; RMSEC, RMSECV, and RMSEP – root mean square errors of calibration, cross-validation, and prediction in original units, RPD – residual predictive deviation.

signal. Table 3 shows the characteristics of regression models for each parameter.

The optimal number of latent variables (LV) was selected based on the analysis of RMSEC and RMSECV as a function of the number of PLS components. The model performance was evaluated on the basis of the determination coefficient, R_{CV}^2 and R_P^2, and the RMSECV and RMSEP for cross-validation and external validation, respectively. Additionally, the utility of the models for the prediction of new samples was evaluated on the basis of the RPD.

We followed the criteria proposed in ref. 39 to evaluate the performance of the regression models. NPLS models based on the analysis of the entire EEMs were characterized by RPD > 2 for TPC, corresponding to moderate predictive accuracy. PLS models based on analysis of unfolded EEMs exhibited good predictive performance for PI and moderate for TPC and V. Other PLS and NPLS models based on the spectral data showed lower predictive performance and were adequate only for screening. Among PLS models based on PARAFAC scores and the Rayleigh scattering signal, moderate predictive performance was obtained for predicting PI and viscosity, while models for other parameters had lower performance. Even if there is no fluorescence data associated with the oxidation products, the developed models were able to predict physicochemical parameters. This is due to the correlation between the concentration of fluorescent components and those parameters.

Based on the analysis of VIP for PLS-PARAFAC-R models, we identified the variables with important contributions to the prediction of respective analytical parameters (ESI, Fig. S2†). Scores of fluorescent components 2, 3, and 4 had important contributions to the prediction of TPC. For predicting PI, IV, and viscosity, the significant impact came from scores of component 4 and the intensity of the Rayleigh scattering signal. For the prediction of AI, the important variables included scores of components 1 and 4, and the intensity of the Rayleigh scattering signal. These results show that, in addition to fluorescence properties, Rayleigh scattering signal analysis may also be useful for modeling the processes occurring during ozonation.

4 Conclusions

The analysis of EEMs of olive oil samples revealed the gradual degradation of all fluorescent components, tocopherols, phenols and pheophytins, as a function of ozonation time. The oxidation products formed during ozonation did not emit any fluorescence, in contrast to the photo- and thermo-oxidation products, whose fluorescence was described in the literature. The developed multivariate models for the prediction of total polyphenol content (TPC) had moderate predictive performance and were adequate for screening analysis. The evaluation of polyphenols during ozonation is important because of the biological activity of ozonated olive oils; as many of the health benefits attributed to these products may be related to the interaction of both polyphenolic substances and peroxidic species.

It was also possible to develop models for the peroxide index (PI) and viscosity (V); however, these models were based on indirect correlation between fluorescent components and respective parameters. Moreover, we demonstrated that the intensity of the Rayleigh scattering signal is highly correlated with the viscosity and peroxide index and may be useful to model these parameters.

In summary, we demonstrated the feasibility of EEM spectroscopy for monitoring the ozonation process; using this method can ease the characterization of ozonated olive oils and, additionally, make the analysis more sustainable. Finally, it is worth mentioning that the two oils studied: virgin olive oil (VOO) and pomace olive oil (POO), showed similar physicochemical characteristics and behaviour during the ozonation treatments. Given that POO is one of the main waste by-products of the olive oil industry, the information obtained is of special interest because it presents new possible applications for POO as an ozonated vegetable oil in both the food industry and clinical treatments.

Data availability

Data will be made available upon request.

Author contributions

Paula Domínguez-Lacueva: methodology, investigation, data curation, formal analysis, software, writing – original draft; Ewa Sikorska: methodology, formal analysis, software, validation; María J. Cantalejo-Díez: conceptualization, supervision, validation, visualization, writing – review and editing, project administration, funding acquisition.

Conflicts of interest

There are no conflicts to declare.

Acknowledgements

This research work has been financially supported by the Government of Navarre (Spain) in the framework of the PROMETEA project (0011-1411-2022-000024). We would like to thank Biosasun S. A. for providing the olive oils used in this study. Also, we would like to thank Asociación Allotarra de Agricultura y Ganadería Ecológica in Navarre, Spain, for providing the open access funding.

References

1 D. Bouzid, S. Merzouki, H. Boukhebti and M. M. Zerroug, *Ozone: Sci. Eng.*, 2021, **43**, 606–612.
2 A. P. Pivotto, F. W. Banhuk, I. V. Staffen, M. A. Daga, T. S. Ayala and R. A. Menolli, *Online J. Biol. Sci.*, 2020, **20**, 37–49.
3 R. Criegee, *Angew Chem. Int. Ed. Engl.*, 1975, **14**, 745–752.
4 J. Zeng and J. Lu, *Int. Immunopharmacol.*, 2018, **56**, 235–241.
5 S. Jbara, A. S. Shehadeh, S. Trefi and Y. Bitar, *Bull. Pharm. Sci.*, 2022, **45**, 249–268.
6 N. Rodrigues de Almeida Kogawa, E. José de Arruda, A. C. Micheletti, M. de Fatima Cepa Matos, L. C. Silva de

Oliveira, D. Pires de Lima, N. C. Pereira Carvalho, P. Dias de Oliveira, M. de Castro Cunha, M. Ojeda and A. Beatriz, *RSC Adv.*, 2013, **5**, 65427–65436.
7 R. Feier, R. M. S. Cucui, R. F. Ratiu, D. Baciu, C. Galea, L. Sachelarie, C. Nistor, D. Cocos, L. L. Hurjui and E. R. Cernei, *Appl. Sci.*, 2023, **13**, 2831.
8 V. F. Georgiev, T. T. Batakliev, M. P. Anachkov and S. K. Rakovski, *Ozone: Sci. Eng.*, 2015, **37**, 55–61.
9 M. Radzimierska-Kaźmierczak, K. Śmigielski, M. Sikora, A. Nowak, A. Plucińska, A. Kunicka-Styczyńska and K. H. Czarnecka-Chrebelska, *Molecules*, 2021, **26**, 3074.
10 M. Díaz, R. Hernández, G. Martínez, G. Vidal, M. Gómez, H. Fernández and R. Garcés, *J. Braz. Chem. Soc.*, 2006, **17**, 403–407.
11 R. Mateos, B. Sarria and L. Bravo, *Crit. Rev. Food Sci. Nutr.*, 2020, **60**, 3506–3521.
12 Y.-L. Huang, M. B. Oppong, Y. Guo, L.-Z. Wang, S.-M. Fang, Y.-R. Deng and X.-M. Gao, *Fitoterapia*, 2019, **136**, 104155.
13 S. Carpi, E. Scoditti, M. Massaro, B. Polini, C. Manera, M. Digiacomo, J. Esposito Salsano, G. Poli, T. Tuccinardi, S. Doccini, F. M. Santorelli, M. A. Carluccio, M. Macchia, M. Wabitsch, R. De Caterina and P. Nieri, *Nutrients*, 2019, **11**, 2855.
14 M. R. Emma, G. Augello, V. Di Stefano, A. Azzolina, L. Giannitrapani, G. Montalto, M. Cervello and A. Cusimano, *Int. J. Mol. Sci.*, 2021, **22**, 1234.
15 V. Pedan, M. Popp, S. Rohn, M. Nyfeler and A. Bongartz, *Molecules*, 2019, **24**, 2041.
16 T. Gutfinger, *J. Am. Oil Chem. Soc.*, 1981, **58**, 966–968.
17 M. Servili and G. Montedoro, *Eur. J. Lipid Sci. Technol.*, 2002, **104**, 602–613.
18 M. Issaoui, G. Flamini, M. E. Hajaij, P. L. Cioni and M. Hammami, *J. Am. Oil Chem. Soc.*, 2011, **88**, 1339–1350.
19 A. Carrasco-Pancorbo, L. Cerretani, A. Bendini, A. Segura-Carretero, G. Lercker and A. Fernández-Gutiérrez, *J. Agric. Food Chem.*, 2007, **55**, 4771–4780.
20 N. Tena, D. L. García-González and R. Aparicio, *J. Agric. Food Chem.*, 2009, **57**, 10505–10511.
21 S. Yalcin and M. Schreiner, *J. Food Sci. Technol.*, 2018, **55**, 244–251.
22 S. Esposto, A. Taticchi, S. Urbani, R. Selvaggini, G. Veneziani, I. Di Maio, B. Sordini and M. Servili, *Food Chem.*, 2017, **229**, 726–733.
23 R. Aparicio-Ruiz, N. Tena, I. Romero, R. Aparicio, D. L. García-González and M. T. Morales, *Grasas Aceites*, 2018, **68**, 219.
24 E. Sikorska, I. V. Khmelinskii, M. Sikorski, F. Caponio, M. T. Bilancia, A. Pasqualone and T. Gomes, *Int. J. Food Sci. Technol.*, 2008, **43**, 52–61.
25 M. Kharbach, M. Alaoui Mansouri, M. Taabouz and H. Yu, *Foods*, 2023, **12**, 2753.
26 H. Zaroual, E. M. El Hadrami and R. Karoui, *Anal. Methods*, 2021, **13**, 345–358.
27 J. Sadowska, B. Johansson, E. Johannessen, R. Friman, L. Broniarz-Press and J. B. Rosenholm, *Chem. Phys. Lipids*, 2007, **151**, 85–91.
28 M. F. Díaz, J. A. Gavín Sazatornil, O. Ledea, F. Hernández, M. Alaiz and R. Garcés, *Ozone: Sci. Eng.*, 2005, **27**, 247–253.
29 D. T. R. Uebele, C. A. Téllez Soto, N. K. A. M. Galvão, C. R. Tim, A. S. da Silva Sobrinho, R. S. Pessoa and L. dos Santos, *Vib. Spectrosc.*, 2022, **123**, 103460.
30 E. Sikorska, I. Khmelinskii and M. Sikorski, in *Evaluation Technologies for Food Quality*, ed. J. Zhong and X. Wang, Woodhead Publishing, 2019, pp. 491–533.
31 M. Zandomeneghi, L. Carbonaro and C. Caffarata, *J. Agric. Food Chem.*, 2005, **53**, 759–766.
32 G. Squeo, F. Caponio, V. M. Paradiso, C. Summo, A. Pasqualone, I. Khmelinskii and E. Sikorska, *J. Sci. Food Agric.*, 2019, **99**, 2513–2520.
33 E. Martín-Tornero, A. Fernández, I. Durán-Merás and D. Martín-Vertedor, *Molecules*, 2022, **27**, 7254.
34 E. Guzmán, V. Baeten, J. A. F. Pierna and J. A. García-Mesa, *Food Chem.*, 2015, **173**, 927–934.
35 IOC Standards, Methods and Guides, 2023, **https://www.internationaloliveoil.org/what-we-do/chemistry-standardisation-unit/standards-and-methods/**, accessed 2024-02-06.
36 C. M. Andersen and R. Bro, *J. Chemometr.*, 2003, **17**, 200–215.
37 S. Wold, M. Sjöström and L. Eriksson, *Chemometr. Intell. Lab. Syst.*, 2001, **58**, 109–130.
38 I.-G. Chong and C.-H. Jun, *Chemometr. Intell. Lab. Syst.*, 2005, **78**, 103–112.
39 B. M. Nicolaï, K. Beullens, E. Bobelyn, A. Peirs, W. Saeys, K. I. Theron and J. Lammertyn, *Postharvest Biol. Technol.*, 2007, **46**, 99–118.
40 M. Antónia Nunes, A. S. G. Costa, S. Bessada, J. Santos, H. Puga, R. C. Alves, V. Freitas and M. B. P. P. Oliveira, *Sci. Total Environ.*, 2018, **644**, 229–236.
41 C. Eun-Ah and L. Young-San, *Korean J. Food Nutr.*, 2014, **27**, 339–347.
42 I. Grigoletto, P. García Salas, E. Valli, A. Bendini, F. Ferioli, F. Pasini, S. Sánchez Villasclaras, R. García-Ruiz and T. Gallina Toschi, *Foods*, 2024, **13**, 285.
43 F. B. R. D. Iorio, A. M. A. Liberatore, I. H. J. Koh, C. Otani and F. F. Camilo, *Ozone: Sci. Eng.*, 2016, **38**, 253–260.
44 A. Lobo-Prieto, N. Tena, R. Aparicio-Ruiz, D. Gonzalez and E. Sikorska, *Foods*, 2020, **9**, 1846.
45 E. Sikorska, I. Khmelinskii and M. Sikorski, in *Olive Oil - Constituents, Quality, Health Properties and Bioconversions*, ed. D. Boskou, InTech, 2012.
46 B. Gandul-Rojas, M. R.-L. Cepero and M. I. Mínguez-Mosquera, *J. Am. Oil Chem. Soc.*, 2000, **77**, 853–858.
47 H. Wang and X. Wan, *Spectrochim. Acta, Part A*, 2021, **248**, 119183.
48 R. P. Monasterio, L. Olmo-García, A. Bajoub, A. Fernández-Gutiérrez and A. Carrasco-Pancorbo, *Int. J. Mol. Sci.*, 2016, **17**, 1627.
49 E. Sikorska, A. Romaniuk, I. V. Khmelinskii, R. Herance, J. L. Bourdelande, M. Sikorski and J. Kozioł, *J. Fluoresc.*, 2004, **14**, 25–35.
50 B. Uysal, *J. Intercult. Ethnopharmacol.*, 2014, **3**, 49–50.
51 K. S. Potter and J. H. Simmons, in *Optical Materials*, ed. K. S. Potter and J. H. Simmons, 2nd edn, Elsevier, 2021, pp. 101–171.